Surrogate Rehabilitative Time Series Data for Image-based Deep Learning

[1,2]Tracey K. M. Lee, Eileen [3]Y.L. Kuah, [4]Kee-Hao Leo,[5]Saeid Sanei, [6]Effie Chew and [7]Ling Zhao

[1]School of Electrical and Electronic Engineering, Singapore Polytechnic, Singapore: tlee@sp.edu.sg
[2]School of Information Technology, Monash University, Malaysia
[3]Department of Aerospace Engineering, University of Glasgow, Singapore.
[4]Rehabilitation Research Institute of Singapore, Nanyang Technological University, Singapore.
[5] School of Science & Technology, Nottingham Trent University, United Kingdom
[6]Division of Neurology, University Medicine Cluster, National University Hospital, Singapore.

ABSTRACT

Big Data comprise the tools to analyse vast stores of data generated by the myriad of powerful, low-cost processors, sensors and networks around us. The spiralling demand for multi-sensored personal communication devices has played a major role in this, producing images and leaving digital trails of transactions and texts to be mined for patterns. Consequently, the cutting edge of data analysis tools has been targeted for images. However the copious amounts of data required to successfully train these tools are not available in several fields such as rehabilitation where there are constraints on data collection. And yet the need for timely clinical assessments grows.

We consider how to address this situation by generating synthetic, surrogate data which preserves many properties of the original. Here we introduce a new application of surrogate time series in a novel classification scheme, compare methods of converting these into images and use a state of the art neural network framework for a successful improvement in classification results.

This is a significant contribution to the art, demonstrating how scarce time series data can be successfully augmented to take advantage of cutting edge analytical tools.

Index terms - *Deep learning, rehabilitation, accelerometer, surrogate data, time series.*

1. INTRODUCTION

The progress of deep learning as a powerful tool in artificial intelligence has been exceptional. Automated tasks such as image recognition and speech transcription achieved super-human results and surpass humans at several board games. The advanced machine learning algorithms used hold the promise of such superhuman performance in many other fields. A confluence of factors is at play here. These involve the demand for personal communication devices, with their image and motion sensors and the underlying electronic networks with which to communicate. These have led to the ubiquity of *social* networks which facilitate widespread sharing of data using the Internet as a backbone technology. Together with other devices like fitness trackers these have driven down the costs and sizes of sensors and processors.

At another end of the computing spectrum, the demand for realistic gaming scenarios has seen the development of massively parallel graphics processing units (GPU).These bring specialized image processing hardware at consumer prices.

Thus, huge amounts of data - principally images, text and speech, are being generated constantly. The value in these data would have gone undiscovered if not for the processing power of GPUs which are harnessed to analyse the data.

The analytic technology we use is based on neural networks (NN) which were formulated in the 1960's, reached a peak in popularity in the 1980's plateaued and is once more athe forefront of artificial intelligence. The technology then could handle only shallow neural networks, with one hidden layer. These have evolved into the deep learning networks of today with multiple hidden layers and various schemes of neuron connection which require copious amounts of data for training. As it is, these large datasets have come about through the proliferation of social and communication networks. The high computation power in the GPUs have allowed reasonable times to analyse these data. Although network architectures have abounded, the cutting edge is in the area of classifying image data where the Convolutional Neural Network (CNN) is especially effective. A benefit of using existing networks is that parameters learnt can be passed on through *transfer learning*, using only a fraction of the training resources to learn and classify similar data.

Thus to take advantage of these advances, it behooves us to transform our data into images. This is a familiar concept as many often, we can see patterns in a graph more easily than a mathematical description. There have been several approaches to transform one dimensional (1D) time series data into images which we will discuss in Sec. 2.

However unlike the huge caches of image data being shared online, this is not always the case for other fields. For example, there are concerns due to privacy, difficulty in data collection, especially in the biomedical field. One way around this is to generate synthetic data. Monte Carlo simulations and statistics laid the foundations for principled generation of such data.

Our work is based on the widely used [1] Action Research Arm Test (ARAT). It is a test of performance designed to measure the recovery of upper limb function subsequent to injury to the cerebral cortex. The ARAT can be used to evaluate treatment outcomes as well as monitor its progress. Furthermore it can be conducted quickly and is also dependable.

Our setup involves implanting sensors into the objects used in rehabilitation for a less intrusive procedure and a more standardized setup.

In Section 2 we describe the motivation for our approach as well as the background material. Section 3 outlines our physical setup followed by the signal analysis theory in Section 4. Our experimental results are presented in Section 5 and we summarize our discussion with conclusions in Section 6.

2. BACKGROUND WORK

In this section we outline the motivation for our work which aims to take advantage of the advances in machine learning for rehabilitative assessments.

978-9-0827-9703-9/19/$31.00 ©2019 IEEE

Synthetic Surrogate Data

In training NNs, there has always been the need for large data. However, wide scale data gathering is not always practicable for reasons of privacy, expense, time among many factors. To overcome some of these limitations, Rubin [2] first proposed to generate synthetic data that have common characteristics with the original data. This can be realised in a parametric way, for example by using a random number generator and ensuring the numbers have the same mean and variance as the original data. Such an example is that of Synthpop [3] which uses regression and decision trees to do so. However generating synthetic time-series data is more involved as it requires fidelity to the temporal sequence of data.

Using specialized NNs such as Generative Adversarial Networks for generating data are still in research. However surrogate time series data have been successfully used for some time now. Lancaster et. al [4] have recently conducted an extensive review of methods to generate them. Surrogate data is a type of synthetic data that uses bootstrapping, resampling from the original data with replacement. It would be simple to just shuffle the time series data randomly and preserve the mean and variance. But to preserve the temporal correlation and power spectra requires a more nuanced approach which Theiler et al. [5] implemented as the Amplitude Adjusted Fourier Transform (AAFT). An improved version, the Iterated AAFT (IAAFT) was proposed by Schreiber and Schmitz [6].

Feature transformation

The CNN has been designed to specifically take advantage of fundamental image features like edges and lines. The many layers of filters at the input detect these features while the deeper layers of the network. There have been much in the literature about transforming 1D data into 2D images to take advantage of the advances in CNN like that of [7] which considers biomedical signals. We look at three methods that have been widely used.

In the work by Tsai et al., [8] they use line graphs as the image input to a NN. This is a time domain approach which does not require much data processing.

Zhang and Oates [9] proposed the idea of Gramian Angular Fields (GAF). They note that the polar graph of time series data can better preserve and display the temporal correlation between time points. These can be considered as a kind of polar based autocorrelation plot which again is a time domain approach.

Analysing a time series using basis functions can yield different insights. For example Fourier based analyses can highlight the frequencies of interest. For signals which have large frequency content changes, the short time Fourier transform (STFT) can represent changes in frequency with time. The wavelet transform is a generalisation of this idea. A basis function called a wavelet, is shifted and scaled and compared to the time series. The continuous wavelet transform (CWT) or the discrete version can be used. These differ in how the scaling parameters are generated.

2.1 Convolutional Neural Networks

The work by Krizhevsky et al.[10] have set the framework for today's deep learning architectures. These use CNNs trained with the help of GPUs. The network they developed is known as AlexNet and it reduced the error rate from 26% to 15.3% in the ImageNet Large Scale Visual Recognition Challenge in 2012 which featured 15 million images in 1000 categories. Although this performance has been bettered, the architecture of the NN used has not changed much.

A benefit of using existing networks is the use of transfer learning. Large networks and large amounts of data still take a long time to train from the beginning. Through transfer learning, it is possible to use a fraction of these resources if the new application data is similar to that used for training the existing network, by just modifying a few parameters. Furthermore AlexNet has been extensively studied applied and adapted, so there is confidence in the results it produces.

2.2 Instrumenting Rehabilitation Assessments

The conduct of rehabilitation needs to have a protocol for their administration to ensure repeatable, quantitative and objective measurements. Presently the prevalence of these tests are scored visually, which interposes a degree of subjectivity and does not allow subtle motions to be noticed. Besides, the unvarying nature of these assessment activities bring on inattentiveness and human errors. All these motivate for automated test monitoring by electronic means, by instrumenting the objects used in these tests.

Yozbatiran et al. [11] regulated the ARAT by specifying the object sizes used as well as the dimensions of the supporting furniture. In addition, they also specified the scoring in terms of the timing and quality of the movements, but these were based on visual observations.

In [12], Lee et al. reported on work done with the instrumented device outlined in this paper, deploying healthy patient simulators. For the sake of continuity in discussion, parts of their paper have been used here.

As mentioned earlier in this section, the wide availability of sensorized consumer devices have lowered the cost of sensors such as gyroscopes and accelerometers built into them. This is true of devices like smart watches, fitness trackers and gaming devices.

In our work, we insert sensors into objects used in rehabilitation as they can sense fine motion and there is no need for a bodily intrusive sensor attachment procedure. Data can be easily captured online as well.

The overall process flow for our proposed system is shown in Fig. 1. Accelerometer motion data captured in a session are manually segmented from sessions into trials. Then outliers due to noise are compensated for. The time series data are then used to generate two types of surrogate data, extending the data by 10 then 100 times to compare the results of greater data augmentation. These are transformed into three types of images and finally input into a Deep Convolutional Neural Network.

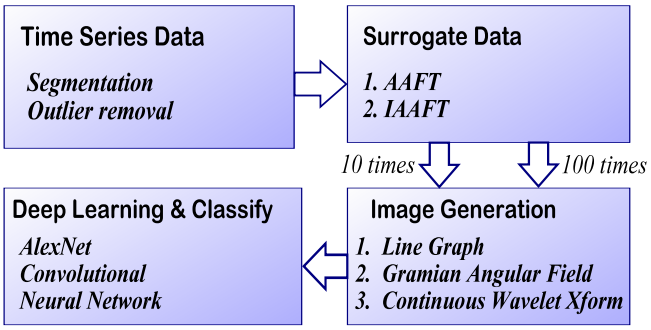

Fig. 1. Processing flow of our rehabilitative time-series data.

We describe our setup in the next section.

3. EXPERIMENTAL SETUP

We outline how Test4 of the ARAT Grasp Subtest is

conducted. This test requires grasping a cube (wooden) measuring 7.5 cm all around. This object which we will term the Cube, is transported from a given point directly to another point. The main sensor of interest is a triaxial accelerometer used to measure motion. The sensor readings are sampled at 30 times per second so that a maximum frequency of 15 Hz can be recorded reliably. Pre-filtering is not done to prevent removing important information and all processing is done in the Matlab® environment.

3.1 ARAT scoring and test subjects

In Fig. 2 we see how the Cube is gripped, held vertically and moved. The ARAT scoring uses a four point scale, from 3 for satisfactory completion to 0 which is non-completion. A score of 3 indicates completion of the task within 5 seconds with appropriate hand, arm and posture movements detailed in [11].

A score of 2 is given when the subject completes the task "with great difficulty and/or takes abnormally long time", from 5 to 60 seconds.

For a score of 1 which indicates partial completion, the timing would be greater than 60 seconds. Also being able to just grasp, hold and lift the Cube would be sufficient to warrant this score.

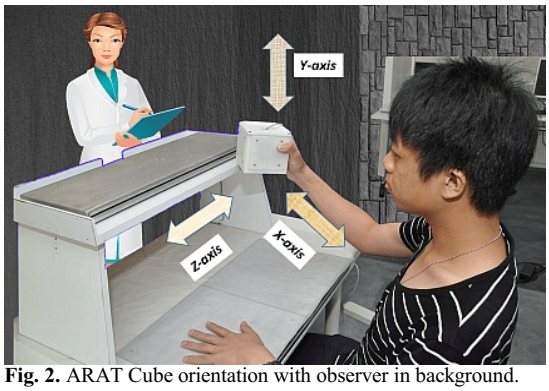

Fig. 2. ARAT Cube orientation with observer in background.

However a score of 0 indicates any of the following: i) inability to perform any part of the task within 60 seconds. ii) inability to grasp the Cube within the time period. iii) subject does not use the fingers to grasp the Cube or use another hand or mechanical support to manipulate the Cube. In all, 34 patients who have had a history of stroke and undergone rehabilitation participated in the trial. This was conducted in a hospital over a period of 60 days. Each patient would perform a set of ARAT motions in one session, up to three times if possible. Each session will have the data is recorded continuously and then segmented manually into its component trials. A significant point to note is that the score is awarded on a *session* basis which implies some kind of averaging is done over the trials. Besides, the sessions were recorded over a period of time and different therapists performed the scoring so some variability is induced in the scores.

From these subjects, 78 trials were recorded. Of these, 31 were scored at 3, 38 scored at 2, 6 scored at 1 and 3 scored at 0, so that there is considerable statistical bias in results. This skew in sample size is probably due to the fitter patients being able to come for trial.

Surrogate data generation

We are not able to determine *a priori* the numbers of patients in each class. It is reasonable to assume equal numbers for a uniform statistical analysis to reduce statistical bias. Thus we generate surrogate data so that each class has roughly the same number of data as shown in Table 1.

Table 1 Table of data set generation. Original then number of surrogates

Score \ Data type	Original	Surrogate×10	Surrogate×100
3	31	310	3100
2	38	380	3800
1	6	360	3600
0	3	360	3600
Total sets	78	1410	14100

4. METHODOLOGY

The theory for surrogate data generation will be described in this section. Then we briefly consider the theory behind some of the 1D to image transforms. Finally we consider structure of the CNN and parameters used. In this section, the time series is represented as a vector $\boldsymbol{x} = \{x_1, x_2 \ldots x_N\}$ of N samples in sequential, equally spaced time intervals.

4.1 Surrogate Data

Surrogate data were originally designed to test for the presence of nonlinearity in a time series. If the underlying model for the time series is not discernible, a nonparametric test is needed. Tests using surrogate data are couched in statistics where the null hypothesis is that the observed time series results from a stochastic, stationary linear process with random inputs. The surrogate data would maintain the stationary properties of the original time series like the mean; in preserving the variance and autocorrelations, this would be reflected in the power spectrum as well. A statistic is computed based on linear considerations in the original data. In computing the same statistic in the surrogates, if there is more variation in values that can be explained by normal variance, then the hypothesis is *rejected*, so that there are possibly nonlinear processes generating the data.

However the *measurement* of the data can introduce nonlinearities and if this is monotonic, this effect can be accounted for. Here we describe the steps, assuming a SORT operator which outputs the sorted data and the indices.

i) $[\{s_i\}\ \{i_{xo}\}] = \mathrm{SORT}(\{x_i\})$; $\{s_i\}$ and $\{i_{xo}\}$ are the sorted data and the corresponding index in $\{x_i\}$ respectively.
$\{i_{rxo}\} = \mathrm{SORT}(\{i_{xo}\})$; $\{i_{rxo}\}$ is the *rank order* of the data, so that $\{s_{i_{rxo}}\} = \{x_i\}$.

ii) $\{r_i\} \in U(0,1)$ where $U(0,1)$ is the uniform distribution generator on the interval [0..1] and $\{r_i\} \in \mathbb{R}$.
$\{p_i\} = \mathrm{SORT}(\{r_i\})$; $\{p_i\}$ are temporary variables.
$\{y_i\} = \{p(i_{rxo})\}$; $\{y_i\}$ are random numbers that have the same *size* distribution as $\{x_i\}$.

iii) $\{Y(\omega)\} = \mathcal{F}(\{y_i\})$; $\{Y(\omega)\}$: Fourier Transform $\mathcal{F}$ of $\{y_i\}$

iv) $\{Y'(\omega)\} = \{Y(\omega)e^{j\varphi}\}$; where the phase $\varphi \in U[0,2\pi)$. $Y'(\omega)$ is the *phase* randomized version of $Y(\omega)$.

v) $\{y'_i)\} = \mathcal{F}^{-1}(\{Y'(\omega)\})$; $\{y'_i\}$ is the time domain version of $\{Y'(\omega)\}$ using $\mathcal{F}^{-1}$.

vi) The input needs to be rank ordered according to the *output* now:
$\{i_{yo}\} = \mathrm{SORT}(\{y'_i\})$; $\{i_{yo}\}$ is the index of the sorted data
$\{i_{ryo}\} = \mathrm{SORT}(i_{yo})$; i_{ryo} is the *rank order* of $\{y'(t)\}$.
$\{x^*_i\} = \{s_{i_{ryo}}\}$; $\{x^*_i\}$ is the surrogate.

The steps comprising the randomized amplitude generation

comprise the AAFT. But this process causes the autocorrelations between the original and surrogates to change. The IAAFT will iterate the surrogate process until there is a close match in the autocorrelations. We illustrate this process with a familiar example of a single cycle sine wave digitized over 12 points.

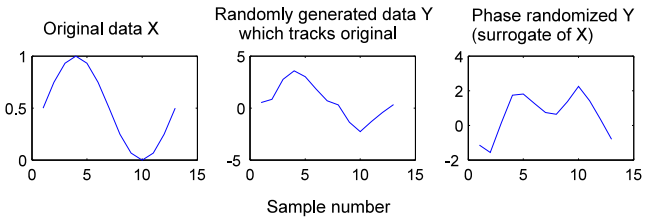

Fig. 3. Illustration of surrogate data generation. Left is original data. Center is randomly generated data which has same rank order as original and right is the phase randomized version which is the surrogate.

4.2 Gramian Angular Field

As mentioned in Sec. 2, the motivation for the GAF is the observation that the temporal relations between points are better preserved in a polar plot. The time series data $\boldsymbol{x}$ are scaled to $\boldsymbol{q}$ whose values fall in the interval $[-1, +1]$.

They are then converted to polar coordinates with the phase $\boldsymbol{\varphi}$ and radius $\boldsymbol{r}$ as:

$$\varphi_i = \cos^{-1} q_i \text{ where } -1 \le q_i \le 1 \text{ for } q \in \boldsymbol{q}$$

$$r_i = i / N \text{ where } i \in \{1...N\}$$

The Gramian Summation Angular Field defines a matrix, where the i^{th}, j^{th} element is given by:

$$cos(\varphi_i + \varphi_j) = cos(\varphi_i)\, cos(\varphi_i) - sin(\varphi_i)\, sin(\varphi_i) \quad i,j \in \{1...N\}$$
$$= q_i q_j + \sqrt{(1 - q^2_i)}\ \sqrt{(1 - q^2_j)} \qquad (1)$$

4.3 Continuous Wavelet Transform Scalogram

A wavelet transform uses a mother wavelet function ψ which has local support. From this function, scaled and translated versions are produced - to be convolved with a signal or time series. The resulting wavelets can be expressed as:

$$1/2^{j/v}\ \psi\ ((i - m)/2^{j/v})$$

where i is the sample number, v is the number of voices per octave, m is the translation parameter. The CWT allows for finer generation of values for the scale $1/2^{j/v}$ and is shift-invariant. Here we use the Morse wavelet which has good time or frequency localized characteristics. It is also analytic, being able to provide instantaneous amplitude, phase and frequency information as well as discussed in [13].

4.4 Convolutional Neural Network

In Fig. 4 we show the overall architecture of AlexNet. It has eight layers, required its input images to be 227 by 227 pixels and was originally trained on 1000 image classes.

Here it is only required to train on 4 classes by which was done by modifying layer 8 only, which is a benefit of transfer learning. We used stochastic descent updates, 20 epochs and a mini-batch size of 64 and an initial learn rate of 0.001.

The original dataset of 78 time series were augmented with 1410 and 14100 sets of surrogate data as described in Table 1. The datasets were combined together and used . We used hold out validation with 80% of the data sets for training and 20% testing chosen randomly and averaged the results for three runs.

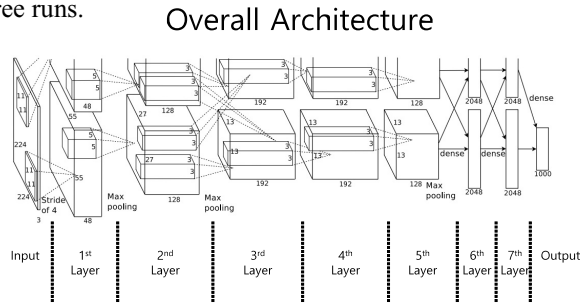

Fig. 4. AlexNet CNN architecture taken from [10].

The training and classifying was done on a Dell XPS 13 (3.4 Ghz capable) with 16 GB RAM using Windows 10.

5. INITIAL ANALYSIS AND RESULTS

In this section we present some initial results of our 1D to 2D image transformations involving surrogate data and the classification results

5.1 Surrogate Time Series Data

The plot of a typical move together with its AAFT and IAAFT surrogates are shown in Fig. 5.

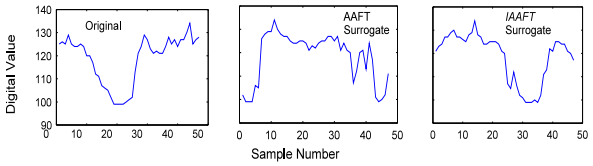

Fig. 5. Plots of original time series (left) followed by AAFT surrogate (center) and IAAFT (right).

5.2 Transformation to Image Features

In this section we show some of the images that result from the transformation of time series into images.

Line graphs

These are the simplest images to generate, being just 1D plots of data against time. Examples of these can be seen in Fig. 5.

Gramian Angular Fields

A typical GAF plot is shown in Fig. 6. This is actually a Gramian Summation Angular Field as described in (1).

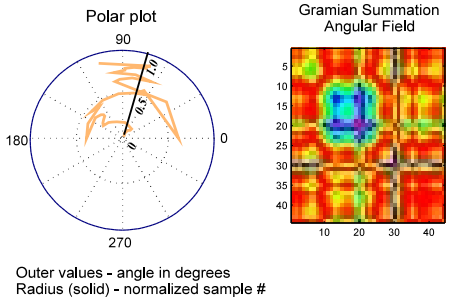

Fig. 6. Gramian Angular Field - left is the polar plot of the time series, right is the Gramian Summation Angular Field.

Due to the nature of the outer product, the evolution of the

time series can be seen in the plot from right half of Fig. 6, progressing from the top left to the bottom right. The diagonal represents the actual time series, with its autocorrelations off-diagonal.

Continuous Wavelet Transform

The plot of frequency to time (or sample number) is known as a scalogram, shown in Fig. 7. The progression of the frequencies of interest with respect to time are clearly shown.

give overall best results as compared to those with some degree of preprocessing as in the GAF and CWT. That the AAFT surrogates work so well show the importance in preserving *time* domain statistics of the original time series which are the mean and variance. In addition, the surrogates also need to preserve the 2nd order *frequency* domain measure which is the power spectrum. In matching the power spectra more accurately, the IAAFT seems to give marginally improved results. Thus we have shown the efficacy of using transfer learning from a state of the art CNN to achieve excellent classification results for automated rehabilitation.

Table 3 Results of classification accuracy with run times in brackets - 80/20 training/validation - averaged over 3 runs

Surrogate	Data Type	Line Graph	Gramian AF	Continuous WT
None	Original data	60.7% (5 mins)	57.6% (5 mins)	46.5% (1 hr)
AAFT	10 × Surrogate	90.1% (16 mins)	86.7% (1 hr)	84.1% (2 hrs)
	100 × Surrogate	100% (5 hrs)	98.9% (19 hrs)	98.5% (12 hrs)
IAAFT	10 × Surrogate	97.1% (25 mins)	86.8% (1.5 hrs)	82.2% (1.5 hrs)
	100 × Surrogate	99.9% (5 hrs)	99.1% (18 hrs)	98.5% (11 hrs)

5.3 Results

In our earlier work [14] we employed hand crafted features to train a decision tree classifier which automatically assigned the ARAT scores with 97.2% accuracy and 72.4% with 21 fold cross validation.

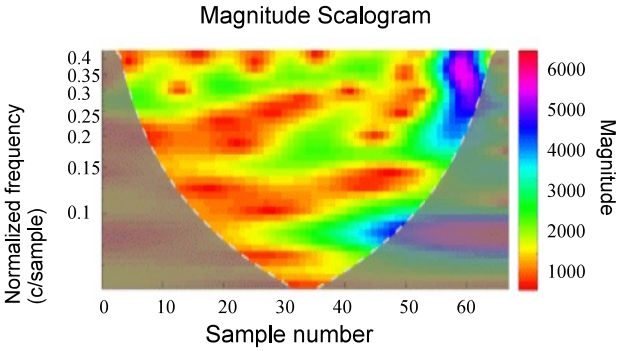

Fig. 7. Scalogram of a typical time-series using a Morse wavelet. Left y-axis shows normalized frequency, right axis - colour map.

In classifying with AlexNet using parameters in Sec. 4.4, we used hold out validation with 80% of the data sets for training and 20% for testing. These were chosen randomly and we averaged the results for three runs. The line graphs show very promising results with the IAAFT and 10 times the amount of surrogate data giving a very high classification rate of 97.1% and with 100 times surrogates, 100%. Furthermore they take up a relatively low amount of time to train.

6. DISCUSSION

In summary we attempted to classify the condition of a subject based on their performance in a subtest from Test4 of the ARAT using data from a triaxial accelerometer. By generating surrogate time series data, transforming them into images and using a pre-trained CNN, we have achieved excellent classification results. It should be noted from Section 3.1 that we are attempting to materialize the basis of what is an essentially subjective rating. This ARAT score is awarded by different scorers over time and not normalized. Based on the motion produced by one subtest, it would seem possible to infer the underlying condition of a subject. This augurs well as a means to assess and assist in the problems associated with a global greying population.

From Table 3, we see that simple time domain images

Subsequent work would involve determining the amount of surrogate data actually needed as well as other types of 1D to image representations. It is also useful to explore other neural network architectures with lower resource demands.

ACKNOWLEDGEMENT

This work was funded by the Ministry of Education of Singapore under grant number 2010MOE-IF-005. We thank Prof D. Kugumtzis and this team for making their software available. We also thank the anonymous reviewers for their comments which have improved the quality of this paper.

REFERENCES

1. L. Santisteban, M. Térémetz, J. Bleton, J. Baron, M. A. Maier and P. G. Lindberg, "Upper limb outcome measures used in stroke rehabilitation studies: A systematic literature review," *PLoS ONE*, 11(5) e0154792, 2016.
2. D. B. Rubin, "Discussion: Statistical Disclosure Limitation," *Journal of Official Statistics*, vol.9, pp.462-468, 1993.
3. B. Nowok, G. Raab and C. Dibben, "synthpop: Bespoke Creation of Synthetic Data in R," *Journal of Statistical Software*, vol.74, no.11, 2016.
4. G. Lancaster, D. Iatsenkob, A. Piddeac, V. Ticcinelli and A. Stefanovska, "Surrogate data for hypothesis testing of physical systems," *Physics Reports*, vol.748, pp.1-60, July 2018.
5. J. Theiler, S. Eubank, A. Longtin, B. Galdrikian and J.D. Farmer, "Testing for nonlinearity in time series: the method of surrogate data," *Physica D: Nonlinear Phenomena* , vol. 58, no.1-4, pp.77-94, 1991.
6. T. Schreiber and R. Schmitz,"Improved Surrogate Data for Nonlinearity Tests", *Physical Review Letters,* vol. 77, pp.635-638, 1996.
7. Y. H. Byeon, S. B. Pan and K. C. Kwak , "Intelligent Deep Models Based on Scalograms of Electrocardiogram Signals for Biometrics," *Sensors*, vol.19, no.4, Feb. 2019.
8. Y. C Tsai, J. H. Chen and J. J. Wang, "Predict Forex Trend via Convolutional Neural Networks," *Journal of Intelligent Systems*, 2018.
9. Z. Wang and T. Oates, "Encoding Time Series as Images for Visual Inspection and Classification Using Tiled Convolutional Neural Networks," *29th AAAI Conference on Artificial Intelligence*, 2015.
10. A. Krizhevsky, I. Sutskever and G. Hinton, "Classification with deep convolutional neural networks," *Proceedings of the Conference on Neural Information Processing Systems (NIPS12)*, 2012.
11. N. Yozbatiran, L. Der-Yeghiaian and S. C. Cramer, "A standardized approach to performing the Action Research Arm Test," *Neurorehabilitation and Neural Repair*, vol.22, no.1, pp.78-90, 2008.
12. T. K. M. Lee, J. G. Lim, S. Sanei, and S. S. W. Gan,"Advances on singular spectrum analysis of rehabilitative assessment data", *J. Med. Imaging Health Inf.,* vol. 5, pp. 350-358, 2015.
13. L. F. Aguiar-Conraria and M. J. Soares, "The continuous wavelet transform: Moving beyond uni- and bivariate analysis," *Journal of Economic Surveys*, vol.28, no.2, April 2014.
14. T. K. M. Lee, J. G. Lim, K. H. Leo, S. Sanei, P. Y. Lew, E. Chew and L. Zhao, "Towards rehabilitative e-Health by introducing a new automatic scoring system," *18th IEEE Healthcom*, Munich, Sep 14-17, 2016.